Current Biology 21, 681–686, April 26, 2011 ©2011 Elsevier Ltd All rights reserved DOI 10.1016/j.cub.2011.03.030

Report

Caveolin-1 Deficiency Causes Cholesterol-Dependent Mitochondrial Dysfunction and Apoptotic Susceptibility

Marta Bosch,[1,11] Montserrat Marí,[2,11] Albert Herms,[1] Ana Fernández,[2] Alba Fajardo,[1] Adam Kassan,[1] Albert Giralt,[3,4] Anna Colell,[2] David Balgoma,[5,6] Elisabet Barbero,[2] Elena González-Moreno,[1] Nuria Matias,[2] Francesc Tebar,[1,3] Jesús Balsinde,[5,6] Marta Camps,[7] Carlos Enrich,[1,3] Steven P. Gross,[8] Carmen García-Ruiz,[2] Esther Pérez-Navarro,[3,4] José C. Fernández-Checa,[2,9,*] and Albert Pol[1,10,*]

[1]Equip de Proliferació i Senyalització Cel·lular, Institut d'Investigacions Biomèdiques August Pi i Sunyer (IDIBAPS), 08036 Barcelona, Spain

[2]Departament de Mort Cel·lular i Proliferació, IDIBAPS, Consejo Superior de Investigaciones Científicas (CSIC) i Unitat d'Hepatologia, Hospital Clínic i Provincial de Barcelona, Centre d'Investigacions Biomèdiques Esther Koplowitz, 08036 Barcelona, Spain

[3]Departament de Biologia Cel·lular, Immunologia i Neurociències, Facultat de Medicina, IDIBAPS, 08036 Barcelona, Spain

[4]Centro de Investigación Biomédica en Red (CIBER) de Enfermedades Neurodegenerativas, Universitat de Barcelona, 08036 Barcelona, Spain

[5]Instituto de Biología y Genética Molecular, CSIC, 47003 Valladolid, Spain

[6]CIBER de Diabetes y Enfermedades Metabólicas Asociadas, 08036 Barcelona, Spain

[7]Departament de Bioquímica i Biologia Molecular, Universitat de Barcelona i Institut de Recerca Biomèdica de Barcelona, Parc Científic, 08028 Barcelona, Spain

[8]Department of Developmental and Cell Biology, University of California, Irvine, Irvine, CA 92697, USA

[9]Research Center for Alcoholic Liver and Pancreatic Diseases, Keck School of Medicine, University of Southern California, Los Angeles, CA 90033, USA

[10]Institució Catalana de Recerca i Estudis Avançats, 08010 Barcelona, Spain

Summary

Caveolins (CAVs) are essential components of caveolae, plasma membrane invaginations with reduced fluidity, reflecting cholesterol accumulation [1]. CAV proteins bind cholesterol, and CAV's ability to move between cellular compartments helps control intracellular cholesterol fluxes [1–3]. In humans, CAV1 mutations result in lipodystrophy, cell transformation, and cancer [4–7]. CAV1 gene-disrupted mice exhibit cardiovascular diseases, diabetes, cancer, atherosclerosis, and pulmonary fibrosis [8, 9]. The mechanism or mechanisms underlying these disparate effects are unknown, but our past work suggested that CAV1 deficiency might alter metabolism: CAV1$^{-/-}$ mice exhibit impaired liver regeneration unless supplemented with glucose, suggesting systemic inefficiencies requiring additional metabolic intermediates [10]. Establishing a functional link between CAV1 and metabolism would provide a unifying theme to explain these myriad pathologies [11]. Here we demonstrate that impaired proliferation and low survival with glucose restriction is a shortcoming of CAV1-deficient cells caused by impaired mitochondrial function. Without CAV1, free cholesterol accumulates in mitochondrial membranes, increasing membrane condensation and reducing efficiency of the respiratory chain and intrinsic antioxidant defense. Upon activation of oxidative phosphorylation, this promotes accumulation of reactive oxygen species, resulting in cell death. We confirm that this mitochondrial dysfunction predisposes CAV1-deficient animals to mitochondrial-related diseases such as steatohepatitis and neurodegeneration.

Results and Discussion

Establishing a functional link between CAV1 and metabolism would provide a unifying theme to explain the myriad pathologies resulting from CAV deficiency [11]. Thus, mouse embryonic fibroblast cells (MEFs) from wild-type (WT) and CAV1$^{-/-}$ mice [12] were treated with 2-deoxyglucose (2-DG), which inhibits glycolysis. 2-DG reduced proliferation (Figure 1A) and dramatically increased cell death of CAV1$^{-/-}$ but not WT MEFs (Figure 1B). Upon nutrient limitation, cells rely primarily on mitochondrial oxidative phosphorylation (OXPHOS) [13]. Thus, we analyzed whether the increased apoptosis in CAV1$^{-/-}$ cells upon glycolysis inhibition might be caused by increased demands on mitochondria. We treated cells with dichloroacetate (DCA) to shift glucose metabolism from lactate production to OXPHOS [14] (see also Figure S1 available online). DCA preferentially promoted apoptosis in CAV1$^{-/-}$ MEFs (Figure 1C), supporting the hypothesis that lethality is related to activation of OXPHOS. Because OXPHOS is a major source of reactive oxygen species (ROS), and because ROSs are apoptogenic triggers, we quantified cellular ROS levels. CAV1$^{-/-}$ MEFs had a significantly higher ROS content (Figure 1D), and DCA treatment enhanced ROS accumulation in CAV1$^{-/-}$ MEFs. The increased ROS was involved in the increased apoptosis, because treatment with the antioxidant Butylated hydroxyanisole (BHA) reduced the proapoptotic effect of DCA (Figure 1C). These results suggest a mitochondrial dysfunction in CAV1$^{-/-}$ cells, which is exacerbated by stimulation of OXPHOS. This sensitivity is not due to unknown additional variations in the genetic background and also occurs in the animal (see also Figures S2 and S3).

How are the CAV1$^{-/-}$ mitochondria altered? Measured by flow cytometry using MitoTracker FM (data not shown) and cellular cytochrome C content (Figure 2G and Figure 4E), mitochondrial content is similar in both cell types. In contrast, the mitochondrial membrane potential ($\Delta\Psi$) was markedly higher in CAV1$^{-/-}$ cells (Figure 1E). The routine flux control ratio reflects how close the routine respiration operates to the respiratory capacity of the electron transport system, and it was markedly higher in CAV1$^{-/-}$ cells (Figure 1F). We then purified mitochondria [15] from CAV1$^{-/-}$ and WT murine liver [16] and quantified function in identical environments.

*Correspondence: checa229@yahoo.com (J.C.F.-C.), apols@ub.edu (A.P.)

[11]These authors contributed equally to this work

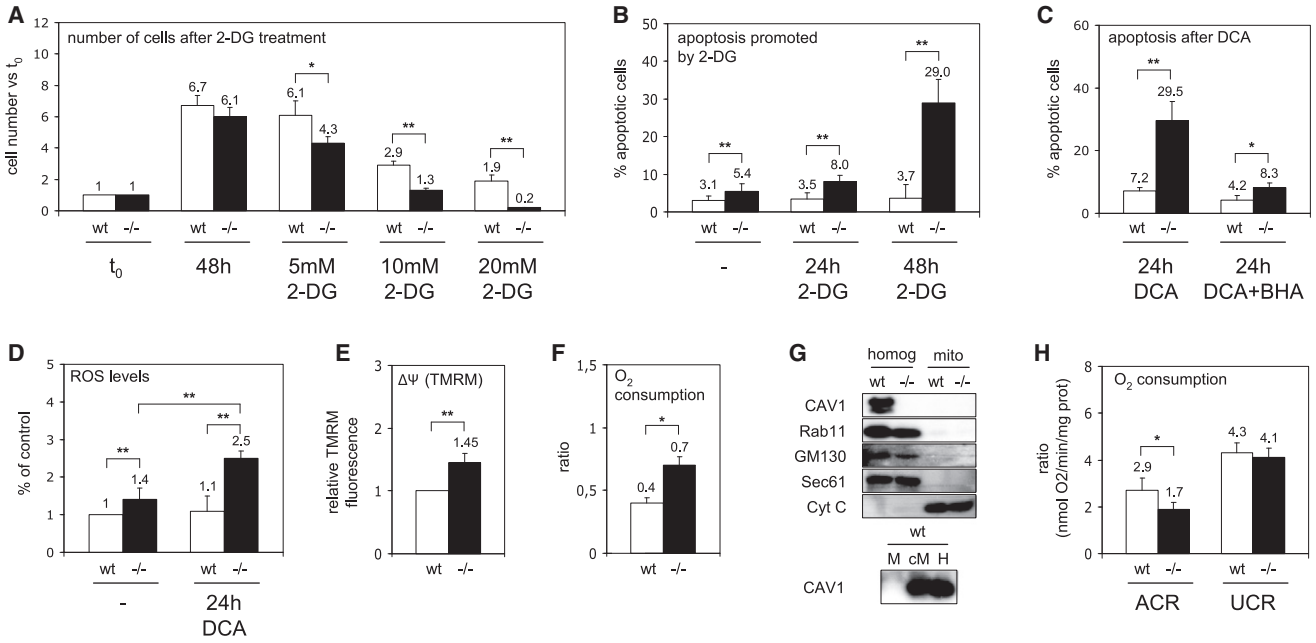

Figure 1. Mitochondrial Dysfunction in CAV1$^{-/-}$ Cells

(A) Wild-type (WT; white bars) and CAV1$^{-/-}$ mouse embryonic fibroblast (MEF; black bars) were cultured with 2-DG. After 48 hr, cell number was determined and expressed with respect to the initial number of cells (t_0).

(B) Apoptosis, analyzed by flow cytometry via binding of annexin V and staining with propidium iodide, was promoted by 5 mM 2-DG.

(C) Apoptosis was promoted by DCA; some cells were pretreated with the antioxidant BHA.

(D) Levels of ROS in cells incubated during 24 hr with DCA. The results are expressed as the relative H2DCFDA fluorescence with respect to untreated WT cells.

(E) $\Delta\Psi$m of CAV1$^{-/-}$ with respect to WT MEF.

(F) Oxygen consumption by WT and CAV1$^{-/-}$ MEF expressed as the routine flux control ratio.

(G) Western blotting analysis of CAV1 (plasma membrane), Rab11 (recycling endosomes), GM130 (Golgi complex), Sec61 (ER), and cytochrome C (Cyt C, mitochondria) in purified WT and CAV1$^{-/-}$ mitochondria (M), in homogenates (H), and in a crude fraction that contains mitochondria and associated ER (cM).

(H) Ratios of oxygen consumption in WT (white bars) and CAV1$^{-/-}$ (black bars) mitochondria purified from mice liver. Statistical significances were determined in at least five independent experiments or ten mice using the Student's t test; *$p < 0.05$, **$p < 0.01$.

The fraction was enriched in cytochrome C and was free of extramitochondrial contamination (Figure 1G). CAV1 was absent in WT mitochondria, though it was present in a crude fraction containing mitochondria and associated endoplasmic reticulum (ER). We determined the respiratory capacity of the purified mitochondria by examining substrate-driven oxygen consumption. The acceptor control ratio (ACR) was calculated to determine the tightness of the coupling between respiration and ATP production, and the uncoupling control ratio (UCR) was calculated as the index of oligomycin-inhibited respiration and FCCP-stimulated respiration. ACR was markedly lower in CAV1$^{-/-}$ mitochondria, whereas the UCR was unaffected (Figure 1H). Thus, CAV1$^{-/-}$ mitochondria show reduced flux between the respiratory chain and the production of energy. The apparent discrepancy of higher mitochondrial potential and higher oxygen consumption observed in CAV1$^{-/-}$ cells deserves further analysis, but because the UCR is unaffected, it is not caused by changes in membrane permeability.

How might CAV1 loss result in mitochondrial impairment? CAV1 contributes to intracellular cholesterol homeostasis [1–3]. CAV1 deficiency might alter mitochondrial cholesterol levels, which regulate the organelle's function and apoptotic susceptibility [15]. CAV1$^{-/-}$ mitochondria had a significant increase (39%) in free cholesterol (Figure 2A) that could not account for the presence of other cholesterol-enriched organelles (Figure 1G). This deficiency is generic: a mitochondrial fraction isolated from CAV1$^{-/-}$ MEFs had a similar increase of 33% (Figure 3A). Mass spectrometry analysis of major lipids revealed no other significant changes in the total amount of phospholipids or in the relative enrichment of each phospholipid (Table S1). Thus, only the cholesterol/phospholipid ratio was altered from 0.79 in WT to 1.00 in CAV1$^{-/-}$ mitochondria.

Mitochondria are cholesterol-poor organelles, and little is known about regulation of their cholesterol influx or efflux [17]. Cholesterol likely reaches mitochondria through specialized ER domains called mitochondrial-associated membranes (MAM) [18]. Because it is a MAM resident protein [19] and transports cholesterol from the ER to the plasma membrane [20], CAV1 could control MAM cholesterol levels. If so, CAV1 loss would influence steroid synthesis. In steroidogenic cells, after synthesis in the ER, cholesterol is transported into mitochondria, and the P450 side chain cleavage enzyme (CYP11A1) converts it to pregnenolone, the steroid precursor. Mitochondrial cholesterol availability is the rate-determining step in steroid biosynthesis [21], so pregnenolone levels indicate the rate of mitochondrial cholesterol influx. Reduction of CAV1 levels in steroidogenic F2-CHO cells stably transfected with CYP11A1 caused a significant increase in pregnenolone biosynthesis (Figure 2B). Similarly, serum steroid concentrations were significantly higher in CAV1$^{-/-}$ mice (Figure 2C), confirming at the systemic level that CAV1 deficiency promotes higher mitochondrial cholesterol influx and thus increases steroid biosynthesis.

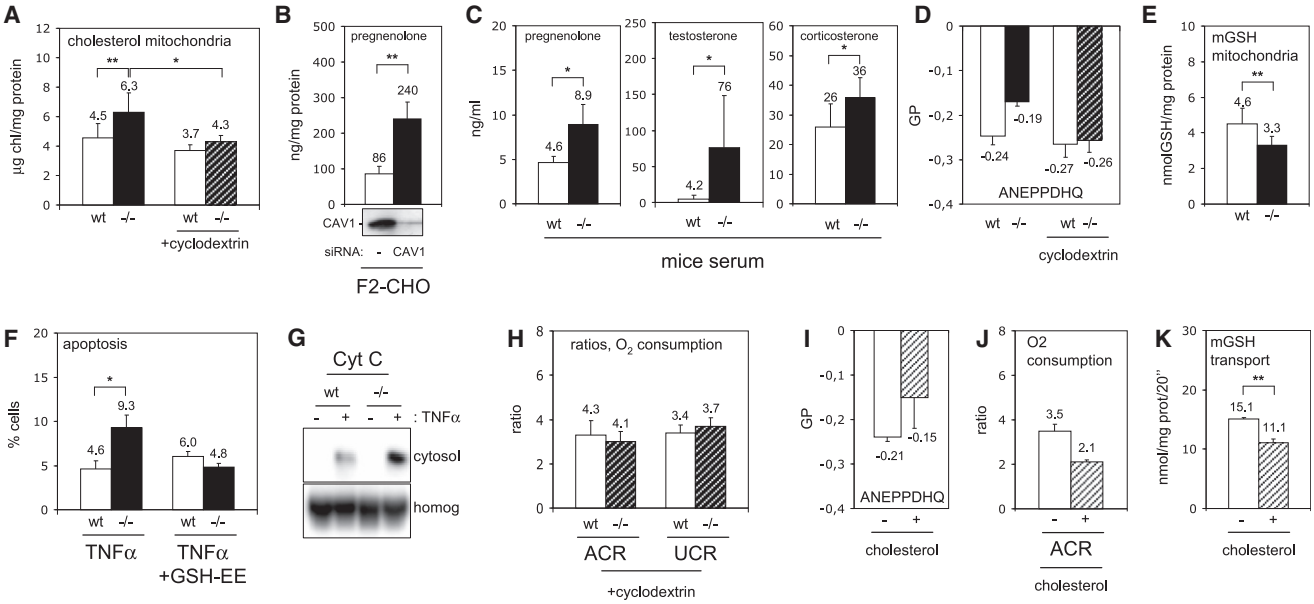

Figure 2. Cholesterol Accumulation Promotes Dysfunction of CAV1$^{-/-}$ Mitochondria

(A) Free cholesterol in WT (white bars) and CAV1$^{-/-}$ (black bars) mitochondria purified from mice liver. In some experiments, mitochondria were pretreated with cyclodextrin to extract cholesterol (slashed bars).

(B) Expression of CAV1 in F2-CHO cells was reduced by RNA interference during 48 hr (western blotting of CAV1 is shown on the bottom), and production of pregnenolone was measured during the next 24 hr.

(C) Pregnenolone, corticosterone, and testosterone levels in the serum of CAV1$^{-/-}$ (black bars) and WT (white bars) mice.

(D) Membrane order analyzed with ANEPPDHQ of WT (white bars), CAV1$^{-/-}$-treated (black bars) and cyclodextrin-treated WT (white bars), and CAV1$^{-/-}$-purified mitochondria (slashed bars).

(E) Mitochondrial GSH in WT (white bars) and CAV1$^{-/-}$ (black bars) mitochondria purified from mice liver.

(F) Apoptosis promoted by 24 hr of TNFα in untreated WT (white bars) and CAV1$^{-/-}$ MEF (black bars) or in cells treated with GSH-EE.

(G) Cytochrome C (Cyt C) in cytosolic supernatants and homogenates (homog) corresponding to TNFα-treated MEFs.

(H) Purified mitochondria from WT (white bars) and CAV1$^{-/-}$ (slashed bars) were treated with cyclodextrin, and the rates of oxygen consumption were measured.

(I and J) Purified WT mitochondria (white bars) were enriched with 25% of cholesterol (slashed bars), and membrane condensation (I) and rates of oxygen consumption (J) were measured.

(K) Influx of a radio-labeled GSH into WT mitochondria untreated (white bars) or enriched with 25% of cholesterol (slashed bars). Statistical significances were determined in at least five independent experiments or ten mice using the Student's t test; *$p < 0.05$, **$p < 0.01$.

In general, cholesterol decreases membrane fluidity, so the mitochondrial cholesterol increase could alter mitochondrial membrane properties. We developed a new technique to measure mitochondrial membrane fluidity and found by di-4-ANEPPDHQ that purified CAV1 $^{-/-}$ mitochondria had increased membrane condensation (Figure 2D and see Supplemental Experimental Procedures). Reduced membrane fluidity impairs import of glutathione into the mitochondria (mGSH) [15]. GSH is a key antioxidant that modulates the oxidative state of the cell and ultimately apoptosis [22]. Indeed, purified CAV1$^{-/-}$ hepatic mitochondria had a 28% reduction in mGSH content (Figure 2E). A mitochondrial fraction isolated from CAV1$^{-/-}$ MEFs also showed a reduction of 59% (Figure 3B). Decreased mGSH partially explains the ROS accumulation in CAV1$^{-/-}$ cells. Mitochondrial GSH reduction predisposes cells to apoptosis [15, 22], and indeed CAV1$^{-/-}$ MEFs displayed significantly higher apoptosis when challenged with TNFα (Figure 2F). The increased apoptosis was confirmed by measuring cytochrome C release into the cytosol (Figure 2G). Using cell-permeable GSH ethyl ester (GSH-EE) to increase mGSH levels eliminated the difference in apoptotic sensitivity between WT and CAV1$^{-/-}$ fibroblasts (Figure 2F).

These data thus support the hypothesis that CAV1 deficiency promotes cholesterol accumulation in mitochondria, reducing membrane fluidity and causing organelle dysfunction by (1) reducing respiratory chain efficiency and increasing ROS levels and (2) reducing uptake of mGSH and thus mitochondrial antioxidant defense. To directly test cholesterol's role, we treated purified CAV1$^{-/-}$ mitochondria with beta-cyclodextrin to extract cholesterol. This restored the cholesterol/phospholipid ratio of CAV1$^{-/-}$ mitochondria to the WT levels without affecting the amount of phospholipids (4.30 ± 1.15 ng cholesterol/mg protein and 6.06 ± 0.76 nmol Pi/µg protein; Figure 2A). Critically, these CAV1$^{-/-}$ mitochondria treated with cyclodextrin had reduced membrane order, as shown by di-4-ANEPPDHQ (Figure 2D), and their ACR index recovered to WT mitochondria levels (Figure 2H). Further, their susceptibility to mitochondrial toxins was reversed (Figure 4I). Conversely, when purified WT mitochondria were loaded with an additional 25% of cholesterol, they demonstrated increased membrane order (Figure 2I), reduced ACR index (Figure 2J), and reduced entry of mGSH (Figure 2K). Re-expression by retroviral infection of CAV1 in CAV1$^{-/-}$ MEF [23] recovered mitochondrial cholesterol and mGSH levels (Figures 3A and 3B), reduced the routine flux control ratio, especially after OXPHOS activation by DCA (Figure 3C), and decreased the oxidative stress caused by DCA as measured by oxidation of Dihydroethidium (DHE) (Figure 3D). In summary, dysfunction in the CAV1$^{-/-}$ mitochondria largely results from increased mitochondrial cholesterol.

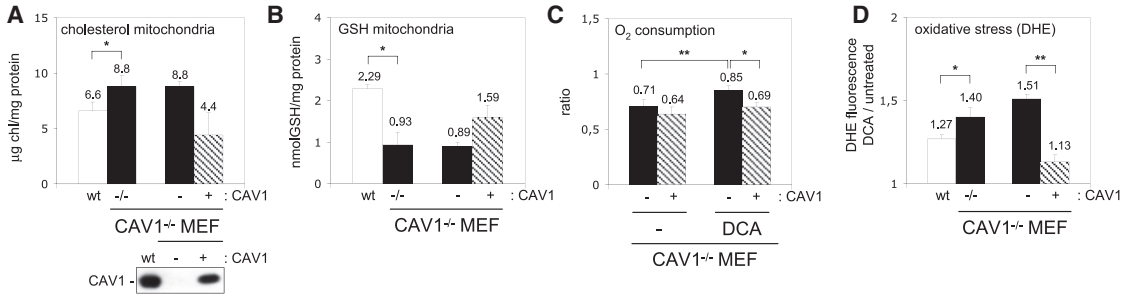

Figure 3. Reexpression of CAV1 Recovers Mitochondrial Function

(A and B) Free cholesterol and GSH in mitochondria purified from WT (white bars), CAV1$^{-/-}$ (black bars), CAV1$^{-/-}$-reconstituted MEFs (slashed bars), and CAV1$^{-/-}$ MEF infected with an empty vector (black bars). CAV1 levels are shown by western blotting.

(C) Routine flux control ratio in untreated MEFs and in cells incubated with DCA for 5 hr.

(D) Oxidative stress caused by mitochondrial function in MEFs. Results are expressed as the ratio between the fluorescence intensity of DHE after treating the cells with DCA for 5 hr with respect to the initial intensity. Statistical significances were determined in at least five independent experiments using the Student's t test; *p < 0.05, **p < 0.01.

Mitochondrial impairment should make CAV1-altered animals sensitive to diseases involving mitochondrial malfunction. Because cholesterol loading of mitochondria is known to sensitize the liver to steatohepatitis [15], CAV1$^{-/-}$ mice should be particularly sensitive to this disease. We treated mice with the agonistic anti-Fas antibody Jo2. Injury was minimal in WT liver, but in CAV1$^{-/-}$ mice Jo2 caused appearance of serum transaminases reflecting hepatic damage (Figure 4A). Steatohepatitis progression was shown by hematoxiline-eosin staining and inflammatory cell infiltration of liver sections (Figures 4B and 4C). The increased susceptibility of CAV1$^{-/-}$ hepatocytes to Jo2 was reproduced in isolated primary hepatocytes (Figures 4D–4F). Importantly, increasing cellular GSH levels by the cell-permeable GSH ethyl ester rescued CAV1$^{-/-}$ hepatocytes from Jo2-induced cell death (Figure 4F).

Mitochondrial impairment and oxidative stress contribute to neuronal death in multiple forms of neurodegeneration [24], and CAV1$^{-/-}$ brain mitochondria also have increased cholesterol levels and reduced mGSH (Figures 4G and 4H). To test whether CAV1 loss also sensitized these mitochondria to typical neurodegenerative insults, we incubated mitochondria with oligomeric human recombinant Aβ1-42 (the amyloid beta peptide [Aβ] characteristic of Alzheimer's disease and a potent mitochondrial toxin [25]). CAV1$^{-/-}$ brain mitochondria had higher ROS generation (Figure 4I) and enhanced cytochrome C release (data not shown). This effect was reversed by extracting mitochondrial cholesterol with cyclodextrin (Figure 4I).

Finally, we tested for mitochondrial dysfunction in the intact brain by injecting 3-Nitropropionic acid (3-NP). This is a mitochondrial toxin used extensively as a model of Huntington's disease; its toxicity is associated with oxidative stress [26]. 3-NP was injected in the striatum of WT and CAV1$^{-/-}$ mice, and degenerating cells were visualized 24 hr later. In the CAV1$^{-/-}$ striatum, we found a much larger lesion (Figure 4J; volume quantified in serial sections), and by staining with TUNEL (Figure 4K), we calculated twice the apoptotic neurons per lesion ($62.3 \times 10^3 \pm 7.6 \times 10^3$ in WT and $133 \times 10^3 \pm 13.5 \times 10^3$ in CAV1$^{-/-}$; **p < 0.01).

In summary, CAV1 deficiency impairs mitochondria by promoting an increased influx and accumulation of free cholesterol in mitochondrial membranes. This increases membrane condensation, decreasing efficiency of the respiratory chain and the intrinsic antioxidant defense. Upon activation of OXPHOS, the combination of these factors promotes accumulation of ROS, resulting in cell death. Although we only investigated the effect of the mitochondrial failure caused by CAV1 deficiency in liver, brain, and fibroblasts, naturally occurring CAV1 deficiencies in humans cause disease in other tissues as well. The precise contribution of the mitochondrial dysfunction in the appearance and/or progression of the pathologies attributed to the loss of CAV should now be addressed in each specific case. In this respect, we have confirmed organismal vulnerability to mitochondrial perturbations occurring during progression of steatohepatitis and neurodegeneration. In a physiological context, cells are continuously exposed to changes in the balance between aerobic glycolysis and mitochondrial oxidative metabolism, so our findings more generally suggest that CAV deficiency will progressively result in mitochondrial failure, sustained oxidative stress, and apoptosis, casually contributing to disease pathogenesis.

Experimental Procedures

Reagents and Antibodies

BHA (B1253), GSH-EE (G1404), DCA (347795), 2-DG (31060, Fluka), insulin (I9278), EGF (E1557), PDGF (P4056), collagenase type IV (C5138), glucose (8270), fatty acids (L9655), and 3-NP (N5636) were from Sigma. Jo2 (554254) was from PharMingen, Hoechst-33258, Deep Red MitoTracker (M22426), MitoTracker green FM (M-7514), and DHE (D11347) were from Molecular Probes, Trypsin/EDTA was from Life Technologies, TNFα (300-01A) was from PeproTech (Bionova), monoclonal anti-cytochrome C (6H2B4) was from BD PharMingen, anti-smac/DIABLO was from Calbiochem, anti-GFP (ab290) was from Abcam, and anti-CAV1 (C13630) and anti-actin were from Transduction Labs.

Cells and Animals

MEFs [12] were grown in Dulbecco's modified Eagle's medium supplemented with 5% fetal bovine serum, L-glutamine (2 mM), penicillin (50 U/ml), and streptomycin sulfate (50 μg/ml) (Biological Industries). F2-CHO, 3T3L1 cells, CAV1$^{-/-}$-reconstituted MEFs, and CAV1$^{-/-}$ MEF stably transfected with the empty vector were obtained and cultured as described [23, 27, 28]. CAV1$^{-/-}$ and WT mice [16] were kept under a controlled humidity and lighting schedule with a 12 hr dark period. All animals received human care in compliance with institutional guidelines regulated by the European Community. A complete description of the experimental procedures can be found in the Supplemental Experimental Procedures.

Statistical Analysis

The statistical significance of differences was determined using the Student's t test; *p < 0.05, **p < 0.01.

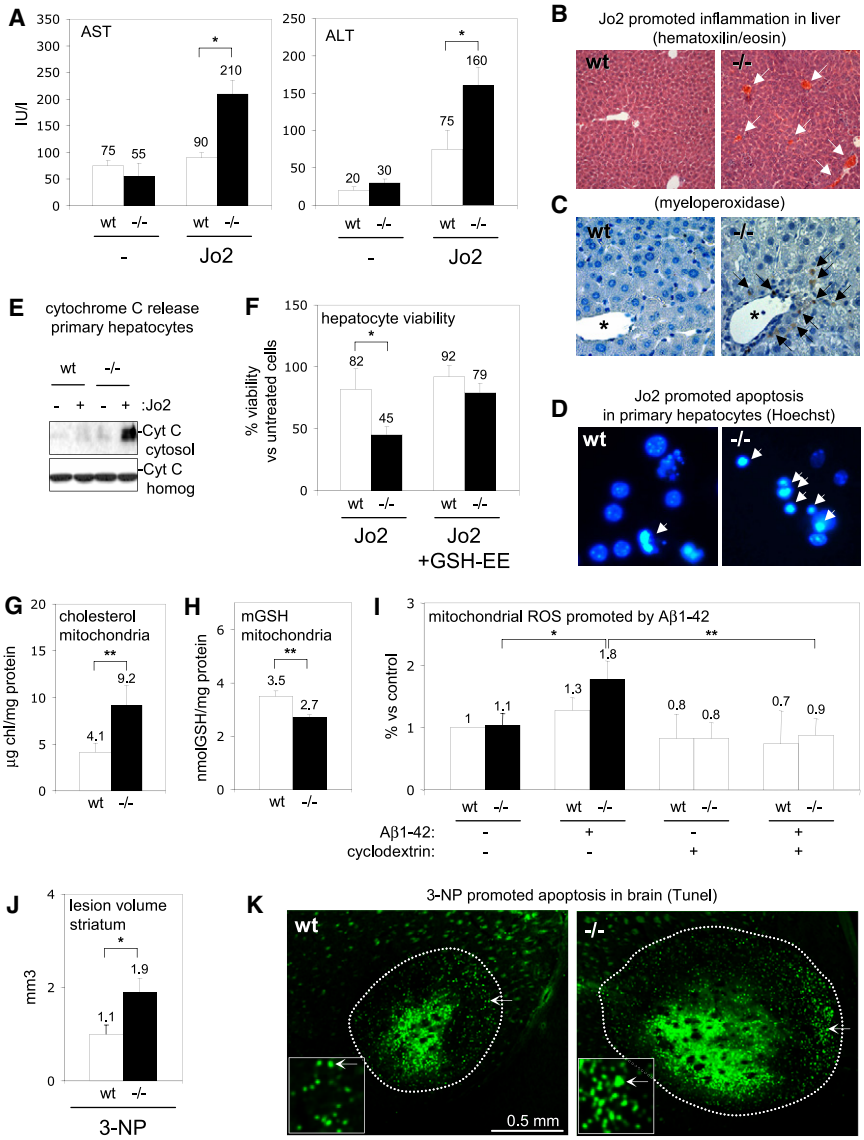

Figure 4. Dysfunction of CAV1$^{-/-}$ Mitochondria Enhances Pathogenesis

(A–C) To model steatohepatitis, we treated WT (white bars) and CAV1$^{-/-}$ (black bars) mice with Jo2. Liver damage was evaluated 24 hr later by appearance of transaminases in serum (AST and ALT). Inflammation was visualized in liver sections of WT (left) and CAV1$^{-/-}$ (right) mice with hematoxiline/eosin and myeloperoxidase staining.

(D and E) WT and CAV1$^{-/-}$ primary hepatocytes were treated with Jo2 for 24 hr. Apoptosis in WT (left) and CAV1$^{-/-}$ (right) hepatocytes was visualized with a Hoechst staining (D) and released cytochrome C (CytC) into the cytosol quantified by western blot (E).

(F) MTT cell viability assay of WT and CAV1$^{-/-}$ hepatocytes treated with Jo2 or with Jo2/GSH-EE.

(G and H) Free cholesterol and mGSH in WT (white bars) and CAV1$^{-/-}$ (black bars) purified brain mitochondria.

(I) ROS generation in WT (white bars) and CAV1$^{-/-}$ (black bars) purified brain mitochondria (some treated with cyclodextrin, slashed bars) incubated with Aβ1-42.

(J and K) 3-NP was injected in the striatum of WT and CAV1$^{-/-}$ mice, and the volume of the lesion measured 24 hr later in serial Fluoro-Jade-stained sections and apoptotic nucleus were visualized in TUNEL-stained sections (K) of WT (left) and CAV1$^{-/-}$ (right) striatum. Statistical significances were determined in at least five independent experiments or ten mice using the Student's t test; *p < 0.05, **p < 0.01.

Supplemental Information

Supplemental Information includes three figures, one table, and Supplemental Experimental Procedures and can be found with this article online at doi:10.1016/j.cub.2011.03.030.

Acknowledgments

A.P. is supported by grants BFU2008-00345, CSD2009-00016, and Marató de TV3, M.M. is supported by grant PI10/02114, A.C. is supported by grant SAF2010-15760, F.T. is supported by grant BFU2006-15474, C.G.-R. is supported by grants SAF2008-02199 and Mutua Madrileña, and C.E. is supported by grants BFU2009-10335 and CSD2009-00016 from Ministerio de Ciencia e Innovación. C.E. is also supported by grant PI040236/Marató TV3, S.P.G. is supported by grant GM64624/NIH, E.P. is supported by grant PI071183, and J.C.F.-C. is supported by grants SAF2009-11417, HI2007-0244/MCI, P50-AA-11999/NIAAA/NIH, and Marató de TV3.We thank Amèrica Giménez and Josep M[a] Marimon from the Animal Facility (Universitat de Barcelona), Maria Calvo and Anna Bosch for help with confocal microscopy (Serveis Cientificotècnics de Barcelona), and Maria Molinos and Susana Nuñez for technical assistance. We also want to thank Barbara Karten (Nova Scotia, Canada) for providing F2-CHO cells.

Received: December 2, 2010
Revised: February 8, 2011
Accepted: March 4, 2011
Published online: April 14, 2011

References

1. Parton, R.G., and Simons, K. (2007). The multiple faces of caveolae. Nat. Rev. Mol. Cell Biol. *8*, 185–194.
2. Pol, A., Luetterforst, R., Lindsay, M., Heino, S., Ikonen, E., and Parton, R.G. (2001). A caveolin dominant negative mutant associates with lipid bodies and induces intracellular cholesterol imbalance. J. Cell Biol. *152*, 1057–1070.
3. Pol, A., Martin, S., Fernández, M.A., Ingelmo-Torres, M., Ferguson, C., Enrich, C., and Parton, R.G. (2005). Cholesterol and fatty acids regulate dynamic caveolin trafficking through the Golgi complex and between the cell surface and lipid bodies. Mol. Biol. Cell *16*, 2091–2105.
4. Cao, H., Alston, L., Ruschman, J., and Hegele, R.A. (2008). Heterozygous CAV1 frameshift mutations (MIM 601047) in patients with atypical partial lipodystrophy and hypertriglyceridemia. Lipids Health Dis. *7*, 3.
5. Kim, C.A., Delépine, M., Boutet, E., El Mourabit, H., Le Lay, S., Meier, M., Nemani, M., Bridel, E., Leite, C.C., Bertola, D.R., et al. (2008).

Association of a homozygous nonsense caveolin-1 mutation with Berardinelli-Seip congenital lipodystrophy. J. Clin. Endocrinol. Metab. *93*, 1129–1134.

6. Lee, H., Park, D.S., Razani, B., Russell, R.G., Pestell, R.G., and Lisanti, M.P. (2002). Caveolin-1 mutations (P132L and null) and the pathogenesis of breast cancer: caveolin-1 (P132L) behaves in a dominant-negative manner and caveolin-1 (-/-) null mice show mammary epithelial cell hyperplasia. Am. J. Pathol. *161*, 1357–1369.
7. Mercier, I., Jasmin, J.F., Pavlides, S., Minetti, C., Flomenberg, N., Pestell, R.G., Frank, P.G., Sotgia, F., and Lisanti, M.P. (2009). Clinical and translational implications of the caveolin gene family: Lessons from mouse models and human genetic disorders. Lab. Invest. *89*, 614–623.
8. Le Lay, S., and Kurzchalia, T.V. (2005). Getting rid of caveolins: Phenotypes of caveolin-deficient animals. Biochim. Biophys. Acta *1746*, 322–333.
9. Cohen, A.W., Hnasko, R., Schubert, W., and Lisanti, M.P. (2004). Role of caveolae and caveolins in health and disease. Physiol. Rev. *84*, 1341–1379.
10. Fernández, M.A., Albor, C., Ingelmo-Torres, M., Nixon, S.J., Ferguson, C., Kurzchalia, T., Tebar, F., Enrich, C., Parton, R.G., and Pol, A. (2006). Caveolin-1 is essential for liver regeneration. Science *313*, 1628–1632.
11. Wallace, D.C., Fan, W., and Procaccio, V. (2010). Mitochondrial energetics and therapeutics. Annu. Rev. Pathol. *5*, 297–348.
12. Razani, B., Engelman, J.A., Wang, X.B., Schubert, W., Zhang, X.L., Marks, C.B., Macaluso, F., Russell, R.G., Li, M., Pestell, R.G., et al. (2001). Caveolin-1 null mice are viable but show evidence of hyperproliferative and vascular abnormalities. J. Biol. Chem. *276*, 38121–38138.
13. Vander Heiden, M.G., Cantley, L.C., and Thompson, C.B. (2009). Understanding the Warburg effect: The metabolic requirements of cell proliferation. Science *324*, 1029–1033.
14. Bonnet, S., Archer, S.L., Allalunis-Turner, J., Haromy, A., Beaulieu, C., Thompson, R., Lee, C.T., Lopaschuk, G.D., Puttagunta, L., Bonnet, S., et al. (2007). A mitochondria-K+ channel axis is suppressed in cancer and its normalization promotes apoptosis and inhibits cancer growth. Cancer Cell *11*, 37–51.
15. Marí, M., Caballero, F., Colell, A., Morales, A., Caballeria, J., Fernandez, A., Enrich, C., Fernandez-Checa, J.C., and García-Ruiz, C. (2006). Mitochondrial free cholesterol loading sensitizes to TNF- and Fas-mediated steatohepatitis. Cell Metab. *4*, 185–198.
16. Drab, M., Verkade, P., Elger, M., Kasper, M., Lohn, M., Lauterbach, B., Menne, J., Lindschau, C., Mende, F., Luft, F.C., et al. (2001). Loss of caveolae, vascular dysfunction, and pulmonary defects in caveolin-1 gene-disrupted mice. Science *293*, 2449–2452.
17. Ikonen, E. (2008). Cellular cholesterol trafficking and compartmentalization. Nat. Rev. Mol. Cell Biol. *9*, 125–138.
18. Hayashi, T., Rizzuto, R., Hajnoczky, G., and Su, T.P. (2009). MAM: More than just a housekeeper. Trends Cell Biol. *19*, 81–88.
19. Sano, R., Annunziata, I., Patterson, A., Moshiach, S., Gomero, E., Opferman, J., Forte, M., and d'Azzo, A. (2009). GM1-ganglioside accumulation at the mitochondria-associated ER membranes links ER stress to Ca(2+)-dependent mitochondrial apoptosis. Mol. Cell *36*, 500–511.
20. Smart, E.J., Ying, Y., Donzell, W.C., and Anderson, R.G. (1996). A role for caveolin in transport of cholesterol from endoplasmic reticulum to plasma membrane. J. Biol. Chem. *271*, 29427–29435.
21. Jefcoate, C. (2002). High-flux mitochondrial cholesterol trafficking, a specialized function of the adrenal cortex. J. Clin. Invest. *110*, 881–890.
22. Montero, J., Mari, M., Colell, A., Morales, A., Basañez, G., Garcia-Ruiz, C., and Fernández-Checa, J.C. (2010). Cholesterol and peroxidized cardiolipin in mitochondrial membrane properties, permeabilization and cell death. Biochim. Biophys. Acta *1797*, 1217–1224.
23. Grande-García, A., Echarri, A., de Rooij, J., Alderson, N.B., Waterman-Storer, C.M., Valdivielso, J.M., and del Pozo, M.A. (2007). Caveolin-1 regulates cell polarization and directional migration through Src kinase and Rho GTPases. J. Cell Biol. *177*, 683–694.
24. Lin, M.T., and Beal, M.F. (2006). Mitochondrial dysfunction and oxidative stress in neurodegenerative diseases. Nature *443*, 787–795.
25. Querfurth, H.W., and LaFerla, F.M. (2010). Alzheimer's disease. N. Engl. J. Med. *362*, 329–344.
26. Brouillet, E., Jacquard, C., Bizat, N., and Blum, D. (2005). 3-Nitropropionic acid: a mitochondrial toxin to uncover physiopathological mechanisms underlying striatal degeneration in Huntington's disease. J. Neurochem. *95*, 1521–1540.
27. Gonzalez-Munoz, E., Lopez-Iglesias, C., Calvo, M., Palacin, M., Zorzano, A., and Camps, M. (2009). Caveolin-1 loss-of-function accelerates GLUT4 and insulin receptor degradation in 3T3-L1 adipocytes. Endocrinology *150*, 3493–3502.
28. Charman, M., Kennedy, B.E., Osborne, N., and Karten, B. (2010). MLN64 mediates egress of cholesterol from endosomes to mitochondria in the absence of functional Niemann-Pick Type C1 protein. J. Lipid Res. *51*, 1023–1034.